Template Synthesis of Stimuli-Responsive Nanoporous Polymer-Based Spheres via Sequential Assembly

Yajun Wang and Frank Caruso*

Centre for Nanoscience and Nanotechnology, Department of Chemical and Biomolecular Engineering, The University of Melbourne, Victoria 3010, Australia

Received April 13, 2006. Revised Manuscript Received June 6, 2006

Nanoporous polymer-based spheres were synthesized via sequential assembly of macromolecules (e.g., polyelectrolytes (PEs), peptides, and proteins) in mesoporous silica (MS) particles, followed by removal of the MS templates. The sequential infiltration of PEs in the mesopores for the model system poly(acrylic acid) (PAA) and poly(allylamine hydrochloride) (PAH) was demonstrated by various methods, including nitrogen sorption, thermogravimetric analysis, Fourier transform infrared, and confocal laser scanning microscopy (CLSM). The influence of parameters such as layer cross-linking, solution pH, ionic strength, and MS pore size on the synthesis of the PAA/PAH nanoporous polymer spheres (NPS) was investigated. Cross-linking between PAA and PAH was found to add structural integrity to the NPS, while the solution pH and ionic strength govern the conformation of the PEs in solution and the subsequent ability of the PEs to infiltrate the mesopores and thereby form intact NPS. Transmission and scanning electron microscopy data show that the PAA/PAH NPS have pores ranging from about 5−50 nm, which was further confirmed by CLSM of protein-loaded NPS. The PAA/PAH NPS exhibited a high capacity for enzyme loading (ca. 470 mg mL^{-1} for lysozyme), with stimuli-responsive reversible loading and release of the protein triggered by changes in solution pH. The general applicability of the reported approach is demonstrated by the preparation of NPS containing peptides, proteins, and low molecular weight molecules. MS fibers were also used as templates to generate PAA/PAH nanoporous fibers, showing that this process is applicable to templates with different morphologies. These nanoporous materials are envisaged to find application in biosensing, enzyme catalysis, and controlled drug delivery.

Introduction

Templating techniques are widely employed to generate advanced materials with tailored properties.[1−12] Various materials with diverse composition, morphology, porosity, and functionality have been synthesized by using natural products (bacteria,[1] cells,[2] diatomite,[3] and starch gel[4]) or synthetic materials (latex spheres,[5] polymer and carbon fibers,[6] and cellulose membranes[7]) as templates. Since its first synthesis in the early 1990s, mesoporous silica (MS) has received widespread interest in template synthesis, mainly owing to its diverse morphologies, high surface area, and tunable porosity.[8] For instance, metal,[9] metal oxide,[10] carbon,[11] and polymer[12] replicas have been prepared through

* Corresponding author. Fax: +61 3 8344 4153. E-mail: fcaruso@unimelb.edu.au.

(1) (a) Davis, S. A.; Burkett, S. L.; Mendelson, N. H.; Mann, S. *Nature* **1997**, *385*, 420. (b) Zhang, B. J.; Davis, S. A.; Mendelson, N. H.; Mann, S. *Chem. Commun*. **2000**, 781.

(2) (a) Chia, S. Y.; Urano, J.; Tamanoi, F.; Dunn, B.; Zink, J. I. *J. Am. Chem. Soc.* **2000**, *122*, 6488. (b) Shin, Y. S.; Liu, J.; Chang, J. H.; Nie, Z. M.; Exarhos, G. *Adv. Mater*. **2001**, *13*, 728. (c) Dong, A.; Wang, Y.; Tang, Y.; Ren, N.; Zhang, Y.; Yue, Y.; Gao, Z. *Adv. Mater.* **2002**, *14*, 926. (d) Towata, A.; Sivakumar, M.; Yasui, K.; Tuziuti, T.; Kozuka, T.; Iida, Y. J. *Ceram. Soc. Jpn.* **2005**, *113*, 696.

(3) (a) Wang, Y.; Tang, Y.; Dong, A.; Wang, X.; Ren, N.; Shan, W.; Gao, Z. *J. Mater. Chem.* **2002**, *12*, 1812. (b) Xu, F.; Wang, Y.; Wang, X.; Zhang, Y.; Tang, Y.; Yang, P. *Adv. Mater*. **2003**, *15*, 1751. (c) Rosi, N. L.; Thaxton, C. S.; Mirkin, C. A. *Angew. Chem., Int. Ed.* **2004**, *43*, 5500. (d) Payne, E. K.; Rosi, N. L.; Xue, C.; Mirkin, C. A. *Angew. Chem., Int. Ed.* **2005**, *44*, 5064.

(4) Zhang, B. J.; Davis, S. A.; Mann, S. *Chem. Mater*. **2002**, *14*, 1369.

(5) (a) Holland, B. T.; Blanford, C. F.; Stein, A. *Science* **1998**, *281*, 538. (b) Holland, B. T.; Blanford, C. F.; Do, T.; Stein, A. *Chem. Mater.* **1999**, *11*, 795. (c) Rhodes, K. H.; Davis, S. A.; Caruso, F.; Zhang, B.; Mann, S. *Chem. Mater*. **2000**, *12*, 2832. (d) Wang, X.; Yang, W.; Tang, Y.; Wang, Y.; Fu, S.; Gao, Z. *Chem. Commun*. **2000**, 2161. (e) Wang, Y.; Tang, Y.; Ni, Z.; Hua, W.; Yang, W.; Wang, X.; Tao, W.; Gao, Z. *Chem. Lett*. **2000**, 510. (f) Caruso, R. A.; Susha, A.; Caruso, F. *Chem. Mater*. **2001**, *13*, 400. (g) Shchukin, D. G.; Caruso, R. A. *Chem. Commun*. **2003**, 1478.

(6) (a) Valtchev, V.; Schoeman, B. J.; Hedlund, J.; Mintova, S.; Sterte, J. *Zeolites* **1996**, *17*, 408. (b) Wang, Y.; Tang, Y.; Wang, X.; Yang, W.; Gao, Z. *Chem. Lett*. **2000**, 1344. (c) Caruso, R. A.; Schattka, J. H.; Greiner, A. *Adv. Mater*. **2001**, *13*, 1577.

(7) (a) Caruso, R. A.; Schattka, J. H. *Adv. Mater*. **2000**, *12*, 1921. (b) Wang, Y.; Tang, Y.; Dong, A.; Wang, X.; Ren, N.; Shan, W.; Gao, Z. *Adv. Mater*. **2002**, *14*, 994. (c) Shchukin, D. G.; Caruso, R. A. *Adv. Funct. Mater*. **2003**, *13*, 789.

(8) Kresge, C. T.; Leonowicz, M. E.; Roth, W. J.; Vartuli, J. C.; Beck, J. S. *Nature* **1992**, *359*, 710.

(9) (a) Liu, Z.; Sakamoto, Y.; Ohsuna, T.; Hiraga, K.; Terasaki, O.; Ko, C. H.; Shin, H. J.; Ryoo, R. *Angew. Chem., Int. Ed.* **2000**, *39*, 3107. (b) Han, Y. J.; Kim, J. M.; Stucky, G. D. *Chem. Mater.* **2000**, *12*, 2068. (c) Lee, K.-B.; Lee, S.-M.; Cheon, J. *Adv. Mater*. **2001**, *13*, 517. (d) Crowley, T. A.; Ziegler, K. J.; Lyons, D. M.; Erts, D.; Olin, H.; Morris, M. A.; Holmes, J. D. *Chem. Mater.* **2003**, *15*, 3518.

(10) (a) Tian, B.; Liu, X.; Yang, H.; Xie, S.; Yu, C.; Tu, B.; Zhao, D. *Adv. Mater.* **2003**, *15*, 1370. (b) Dong, A.; Ren, N.; Tang, Y.; Wang, Y.; Zhang, Y.; Hua, W.; Gao, Z. *J. Am. Chem. Soc.* **2003**, *125* , 4976.

(11) (a) Ryoo, R.; Joo, S. H.; Jun, S. *J. Phys. Chem. B* **1999**, *103*, 7743. (b) Ryoo, R.; Joo, S. H.; Kruk, M.; Jaroniec, M. *Adv. Mater*. **2001**, *13*, 677. (c) Yu, C.; Fan, J.; Tian, B.; Zhao, D.; Stucky, G. D. *Adv. Mater*. **2002**, *14*, 1742.

(12) (a) Goltner, C. G.; Henke, S.; Weissenberger, M. C.; Antonietti, M. *Angew. Chem., Int. Ed.* **1998**, *37*, 613. (b) Kageyama, K.; Tamazawa, J.-I.; Aida, A. *Science* **1999**, *285*, 2113. (c) Kim, J. Y.; Yoon, S. B.; Kooli, F.; Yu, J. *J. Mater. Chem.* **2001**, *11*, 2912. (d) Yilmaz, E.; Ramsrtöm, O.; Möller, P.; Sanchez, D.; Mosbach, K. *J. Mater. Chem.* **2002**, *12*, *1577*.

10.1021/cm060866p CCC: $33.50
Published on Web 07/28/2006

infiltration of low molecular weight precursors in the MS templates, followed by chemical reactions and template removal.

For over a decade, the layer-by-layer (LbL) technique has attracted attention as a method to prepare multilayered thin films with tailored properties on the nanometer scale.[13] The technique exploits the sequential adsorption of oppositely charged materials (e.g., polymers, enzymes, proteins, nanoparticles, and dye molecules) from solution onto charged supports to construct films with tunable composition, thickness, and structure.[13] As a result, the LbL method has been demonstrated to be a simple and effective method for the construction of complex thin films[14] and colloids[15−17] with well-defined properties and for the preparation of polymeric capsules after removal of the core particles.[15−17] Recently, the technique has also been extended beyond conventional planar substrates[13,14] (e.g., silicon and quartz slides and gold electrodes) and colloids[15−17] (e.g., silica and polymer beads) to porous substrates, such as macroporous inorganic oxides,[18] polycarbonate membranes,[19] alumina membranes,[20] and porous calcium carbonate microparticles,[21] to prepare porous polyelectrolyte (PE) structures and tubes. Enhanced properties can be achieved by LbL assembly of PEs on the surface of MS particles preloaded with enzymes[22] or small molecule drugs[23] and, under appropriate solution conditions, within the pores of MS particles to generate nanoporous polymeric spheres (NPS) following removal of the silica template.[24]

Herein, we report that the LbL-template synthesis strategy can be generalized to prepare NPS of diverse composition, morphology, and function via the sequential solution assembly of PEs, (bio)macromolecules, and/or small molecules in MS matrixes. Because it is well-established that the solution conditions play an important role in determining the size and conformation of charged macromolecules in solution,[25] and given that the primary step in the formation of the NPS is the infiltration of the macromolecules in the porous silica matrix, the influence of parameters such as pH and salt in the adsorption solutions is examined. We also investigate the role of cross-linking each layer of material deposited with regard to structural integrity of the NPS. It is demonstrated that this method is applicable to a broad range of materials, generating a suite of porous polymer-based materials containing peptides, proteins, and small molecular weight compounds. Additionally, the nanoporous materials can be prepared with tailored morphologies (spheres, fibers, etc.) and properties, including pH reversible loading and release characteristics for enzymes.

Experimental Section

Materials. Poly(acrylic acid) (PAA, M_w 2 000 g mol^{-1} (acid form) and 30 000 g mol^{-1} (salt form)), poly(allylamine hydrochloride) (PAH, M_w 15 000 and 70 000 g mol^{-1}), poly(L-glutamic acid) (PGA, M_w 1 500−3 000 g mol^{-1}), poly(L-lysine) hydrobromide (PLL, M_w 4 000−14 600 g mol^{-1}), poly(4-styrenesulfonic acid-*co*-maleic acid) sodium salt with a mole ratio 1:1 and 3:1 SS/MA (PSSMA 1:1, M_w 20 000 g mol^{-1}; PSSMA 3:1, M_w 20 000 g mol^{-1}), ethylenediamine (EDA), 1-ethyl-3-(3-dimethylaminopropyl)carbodiimide hydrochloride (EDC), fluorescein isothiocyanate (FITC), hydrofluoric acid (HF), cetyltrimethylammonium bromide (CTABr), 3-aminopropyltriethoxysilane (APTS), *n*-hexadecylamine, sodium metasilicate (Na_2SiO_3), tetraethyl orthosilicate (TEOS, 98%), ammonia solution (25 wt % in water), 2-propanol, dimethyl sulfoxide (DMSO), and sodium chloride (NaCl) were obtained from Sigma-Aldrich and used as received. Lysozyme was purchased from Fluka BioChemika. Phosphate buffer (PB) solutions of pH 2, 7, 5.5, and 8 were prepared using 0.05 M disodium hydrogen phosphate (Na_2HPO_4) and by adjusting the pH with 0.1 M hydrochloric acid (HCl) or sodium hydroxide (NaOH). PE solutions were prepared by dissolving the respective polymers in Milli-Q water at a concentration of 5 mg mL^{-1} and, as required, adjusting the pH with 0.1 M HCl or NaOH. Two main experimental conditions were used for the PAA/PAH systems: the first where the pH was not adjusted (PAA M_w 2 000 g mol^{-1}, pH 2.9, PAH M_w 15 000 g mol^{-1}, pH 4.3) and the second where the pH was fixed at 4.5 (PAA M_w 30 000 g mol^{-1}, PAH M_w 15 000 and 70 000 g mol^{-1}). FITC-labeled lysozyme and PAH were prepared by adding 0.3 mL of a 1 mg mL^{-1} FITC/DMSO solution to 4.0 mL of a 1.0 mg mL^{-1} lysozyme or PAH solution in pH 8.0 PB and allowing it to stand at 20 °C for 45 min. The suspension was then dialyzed against pH 7.0 PB for 72 h, changing the solution every 24 h. The water used in all experiments was prepared in a Millipore Milli-Q purification system and had a resistivity higher than 18 MΩ cm.

MS Template Preparation. The bimodal MS spheres and fibers were prepared according to a literature method.[26] Briefly, 1.38 × 10^{-2} mol of CTABr and 2.1 × 10^{-2} mol of Na_2SiO_3 were dissolved to form a clear solution in 90 mL of Milli-Q water at 30 °C. A total of 6.4 mL and 2.8 mL of ethyl acetate were then added for the sphere and fiber syntheses, respectively. The mixture was stirred for 30 s and allowed to stand at ambient temperature (20 °C) for 5 h. After this period of aging, the bottle was kept at 90 °C for 48 h in an oil bath. The as-prepared silica spheres and fibers with bimodal mesoporous structures are denoted as BMS and FBMS, respectively. The MS spheres with only small mesopores in the range 2−3 nm (denoted as HMS) were prepared using *n*-hexadecylamine as a template in a homogeneous phase of the water/alcohol cosolvent system.[27] Typically, 0.22 g of *n*-hexadecylamine was dissolved in

(13) (a) Decher, G.; Hong, J. D. *Ber. Bunsen-Ges.* **1991**, *95*, 1430. (b) Decher, G. *Science* **1997**, *277*, 1232.
(14) (a) Tedeschi, C.; Caruso, F.; Möhwald, H.; Kirstein, S. *J. Am. Chem. Soc.* **2000**, *122*, 5841. (b) Mamedov, A. A.; Belov, A.; Giersig, M.; Mamedova, N. N.; Kotov, N. A. *J. Am. Chem. Soc.* **2001**, *123*, 7738. (c) Jin, W.; Shi, X.; Caruso, F. *J. Am. Chem. Soc.* **2001**, *123*, 8121.
(15) Caruso, F.; Caruso, R. A.; Möhwald, H. *Science* **1998**, *282*, 1111.
(16) Donath, E.; Sukhorukov, G. B.; Caruso, F.; Davis, S. A.; Möhwald, H. *Angew. Chem., Int. Ed.* **1998**, *37*, 2201.
(17) (a) Caruso, F. *Adv. Mater.* **2001**, *13*, 11. (b) Caruso, F. *Chem.—Eur. J.* **2000**, *6*, 413.
(18) (a) Wang, D.; Caruso, F. *Chem. Commun.* **2001**, 489. (b) Wang, Y.; Caruso, F. *Adv. Funct. Mater.* **2004**, *14*, 1012.
(19) Liang, Z.; Susha, A. S.; Yu, A.; Caruso, F. *Adv. Mater.* **2003**, *15*, 1849.
(20) (a) Ai, S.; Lu, G.; He, Q.; Li, J. *J. Am. Chem. Soc.* **2003**, *125*, 11140. (b) Hou, S.; Harrell, C.; Trofin, L.; Kohli, P.; Martin, C. R. *J. Am. Chem. Soc.* **2004**, *126*, 5674.
(21) (a) Volodkin, D. V.; Petrov, A. I.; Prevot, M.; Sukhorukov, G. B. *Langmuir* **2004**, *20*, 3398. (b) Sukhorukov, G. B.; Volodkin, D. V.; Günther, A. M.; Petrov, A. I.; Shenoy, D. B.; Möhwald, H. *J. Mater. Chem.* **2004**, *14*, 2073.
(22) (a) Wang, Y.; Caruso, F. *Chem. Commun.* **2004**, 1528. (b) Wang, Y.; Caruso, F. *Chem. Mater.* **2005**, *17*, 953. (c) Yu, A.; Wang, Y.; Barlow, B.; Caruso, F. *Adv. Mater.* **2005**, *17*, 1737. (d) Wang, Y.; Caruso, F. *Adv. Mater.* **2006**, *18*, 795.
(23) Zhu, Y. F.; Shi, J. L.; Shen, W. H.; Dong, X. P.; Feng, J. W.; Ruan, M. L.; Li, Y. S. *Angew. Chem., Int. Ed.* **2005**, *44*, 5083.
(24) Wang, Y.; Yu, A.; Caruso, F. *Angew. Chem., Int. Ed.* **2005**, *44*, 2888.
(25) Reith, D.; Müller, B.; Müller-Plathe, F.; Wiegand, S. *J. Chem. Phys.* **2002**, *116*, 9100.
(26) Schulz-Ekloff, G.; Rathouský, J.; Zukal, A. *Int. J. Inorg. Mater.* **1999**, *1*, 97.

Scheme 1. Schematic Representation of the Preparation of NPS by Templating MS Spheres[a]

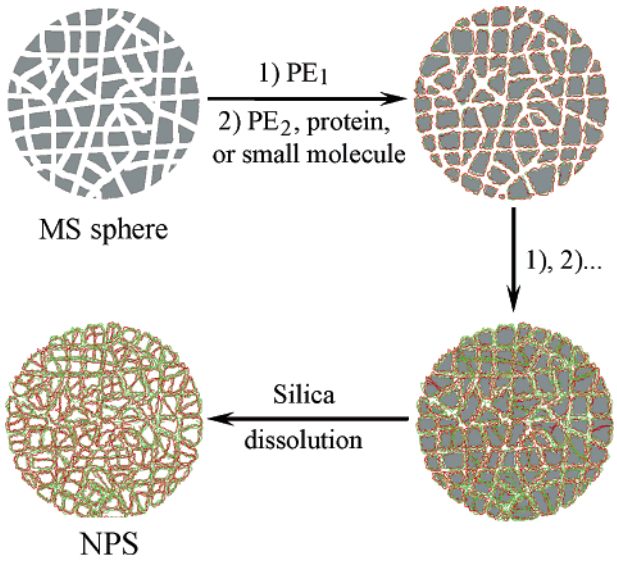

[a] LbL adsorption of macromolecules (PEs, proteins, or small molecular weight molecules) in the mesopores followed by removal of the silica particle template (with HF) yields nanoporous spheres. Thermal or chemical cross-linking can be applied to enhance structural integrity of the nanoporous spheres (see text for details).

a mixture of 25.5 mL of 2-propanol, 0.57 mL of ammonium solution, and 22.8 mL of Milli-Q water to form a clear solution under sonication for 10 min. A total of 1.0 mL of TEOS was then added to this solution under rapid stirring for 10 min, and the mixture was kept standing for 24 h at room temperature.

The as-synthesized particles were collected by centrifugation and washed with ethanol three times and then twice with Milli-Q water. After air-drying at room temperature, the particles were heated at 500 °C for 5 h to remove the surfactants. The MS templates were then functionalized with a layer of primary amine groups by APTS grafting. In this process, the heated particles were dispersed in toluene by sonication for 20 min before APTS was added to the suspension. The molar ratio of the MS particles (calculated as SiO_2)/APTS/toluene was fixed at 5:1:500, and the suspension was refluxed for 24 h. The APTS-grafted MS particles were separated from the solution by centrifugation and washed in toluene and methanol twice. Finally, the pellet was dried at 80 °C for 12 h. The APTS-modified BMS, FBMS, and HMS particles are denoted as APTS-BMS, APTS-FBMS, and APTS-HMS, respectively.

Preparation of Nanoporous Polymer-Based Spheres (NPS). As depicted in Scheme 1, the NPS were prepared by using MS spheres as templates. The chemical structures of some of the building blocks used for the NPS synthesis are shown in Figure 1. Generally, the preparation involves two main steps. The first step entails the sequential deposition of macromolecules within MS templates and optionally cross-linking the layers by heating or by treatment with EDC. A total of 10 mg of the MS particles was dispersed in 2 mL of the PE (5 mg mL^{-1}, various pH and salt conditions, see later in the text), lysozyme (5 mg mL^{-1}, in 50 mM PB at pH 7.0), or EDA (60 mg mL^{-1} in water) solution. Adsorption was conducted by shaking the mixture for 24 h (PE), 72 h (lysozyme), or 2 h (EDA) at 20 °C. Excess PE, lysozyme, and EDA were removed by four cycles of centrifugation (500*g* for 3 min) and washing with 0.1 M NaCl and water. The heat-induced cross-linking was performed by heating the dried sample at 160 °C for 2 h. EDC-induced cross-linking was performed by dispersing the particles in a stirred 0.5 mL EDC solution (60 mg mL^{-1} in 50 mM PB, pH 5.5) for 2 h at 20 °C. In the second step, the MS templates were removed by exposure to 1 mL of 5 M HF solution at 20 °C for 30 min. [*Caution: Extreme care should be taken when handling HF solution.*] NPS were then collected after three centrifugation (1500*g* for 5 min)/water washing cycles.

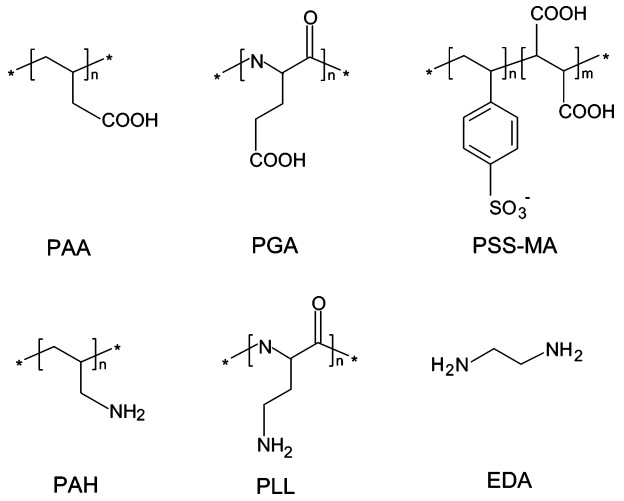

Figure 1. Chemical structures of the PEs, polypeptides, and EDA used in the synthesis of the nanoporous materials.

Reversible Loading of the NPS. The loading and release properties of the NPS were investigated via the adsorption and desorption of lysozyme using the PAA/PAH NPS. For the protein loading, approximately 10 mg of the NPS was dispersed in 15 mL of a 1 mg mL^{-1} lysozyme solution containing 50 mM PB (pH 7.0). The release experiments were performed by dispersing the enzyme-loaded particles in 15 mL of PB solution (50 mM) at pH 2.0. The amount of enzyme loaded or released by the NPS was determined spectrophotometrically by measuring the difference in the supernatant absorbance at 280 nm before and after loading/release.

Instrumentation. Scanning electron microscopy (SEM, Philips XL30, operated at 20 kV) and transmission electron microscopy (TEM, Philips CM120 BioTWIN, operated at 120 kV) were used to examine the morphologies of the NPS. The ultramicrotomed samples were sliced to a thickness of ~90 nm after embedding the NPS in a LR-white resin. Energy-dispersive X-ray (EDX) spectra were obtained on a Philips XL 30 SEM instrument equipped with EDX capability. Fourier transform infrared (FTIR) spectra were recorded on a Varian 7000 FTIR spectrometer. A HP 8453 UV−vis spectrophotometer (Agilent, Palo Alto, CA) was used to monitor the protein loading and release. ζ-potentials were measured on a Zetasizer 2000 (Malvern) instrument, and measurements were conducted in aqueous solutions with no added electrolyte. Confocal laser scanning microscopy (CLSM) images were taken with a Leica DMIRE2 confocal system. Adsorption−desorption measurements were conducted on a Micromeritics Tristar/surface area and porosity analyzer at 77 K using nitrogen as the adsorption gas. The samples were degassed at 120 °C for 12 h before measurement. The surface areas were calculated by the Brunauer−Emmett−Teller (BET) method. Thermogravimetric analysis (TGA) was performed on a Mettler Toledo/TGA/SDTA851e Module analyzer. The samples were heated from 25 °C to 120 °C with a heating rate of 5 °C min^{-1} and kept at 120 °C for 20 min under nitrogen (30 mL min^{-1}). They were then heated from 120 °C to 550 °C with a heating rate of 10 °C min^{-1} under oxygen (30 mL min^{-1}).

(27) Grun, G.; Buchel, C.; Kumar, D.; Schumacher, K.; Bidingmaier, B.; Unger, K. K. *Stud. Surf. Sci. Catal.* **2000**, *128*, 155.

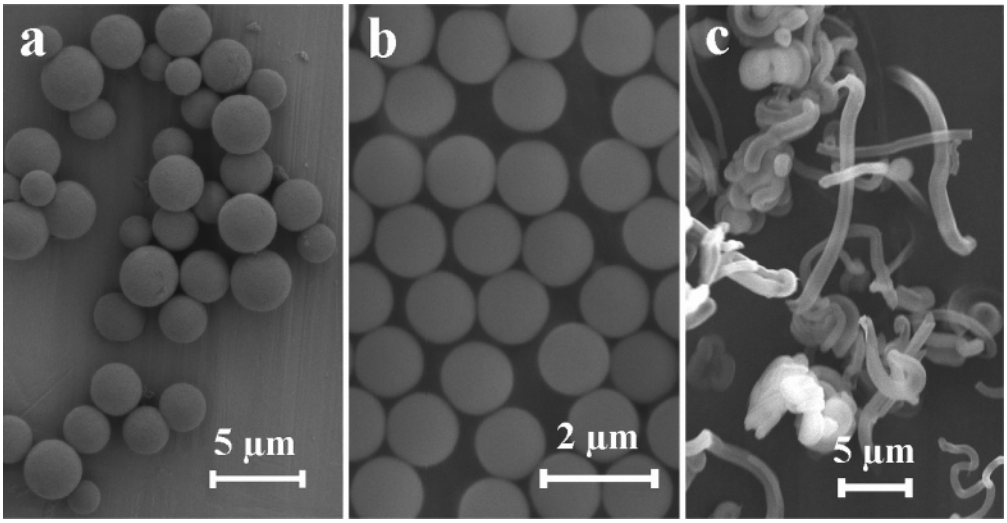

Figure 2. SEM images of the (a) APTS-BMS, (b) APTS-HMS, and (c) APTS-FBMS templates.

Table 1. Properties of the APTS-Modified MS Particles and Fibers Used for Template Synthesis of the Nanoporous Materials

					pore volume, $cm^3\ g^{-1}$	
template	morphology	average size, μm	surface area, $m^2\ g^{-1}$	average pore size, nm	<10 nm[b]	>10 nm[c]
APTS-BMS	sphere	2−3	465	2.6, 10−40[a]	0.32	1.01
APTS-FBMS	fiber	~1 × 10−30	580	2.9, 10−40[a]	0.40	0.66
APTS-HMS	sphere	1.2 ± 0.1	800	2.3	0.65	negligible

[a] Bimodal pore distribution. [b] Total pore volume for pore sizes less than 10 nm. [c] Total pore volume for pore sizes larger than 10 nm.

Results and Discussion

MS Templates. Three types of MS templates with different porosity and morphology were used in the preparation of the nanoporous materials. The MS materials were first functionalized with a layer of amine groups by grafting APTS to the particle surface. Figure 2 shows SEM images of the different APTS-modified templates, the properties of which are summarized in Table 1. The APTS-BMS template has a relatively wide size distribution from ~1.5 to 5 μm, with around 90% of the particles within 2−3 μm. The APTS-HMS templates have an average particle size of 1.2 μm. The APTS-FBMS possesses a fibrous morphology with a diameter of about 1 μm and length of 10 ~ 30 μm. Both the APTS-BMS and the APTS-FBMS have smaller pores in the 2−3 nm range and larger pores ranging from 10 to 40 nm. We chose the APTS-BMS particles as templates to conduct a detailed investigation of the model system PAA/PAH and the parameters that influence the preparation of the NPS.

Infiltration of PAA/PAH in APTS-MS. A facile approach for infiltration of PE into the MS particles is to exploit electrostatic interactions between the MS template and the charged polymers through solution assembly. In this process, oppositely charged PEs, PAA and PAH (Figure 1) are sequentially deposited within the APTS-BMS spheres, with subsequent cross-linking between each PE layer by heating or EDC treatment. The cross-linking treatment promotes amide bond formation between the −COOH groups (in PAA) and the $-NH_2$ moieties (in PAH or on the APTS-BMS template), which stabilizes the PEs infiltrated in the nanopores. Figure 3 shows that the APTS-modified BMS particles exhibit a positive surface charge (>30 mV) over a pH range of 1−7. This facilitates the adsorption of PAA (polyanion) as the first layer through electrostatic interactions. Chemical

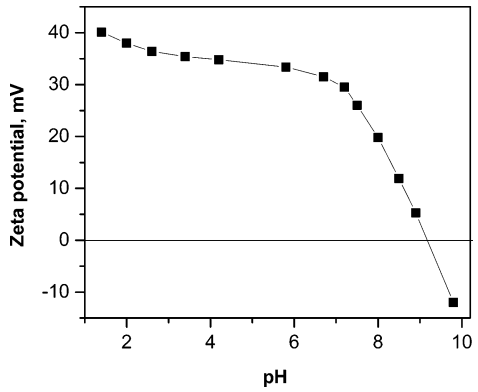

Figure 3. ζ-potential versus pH titration data for the APTS-BMS particles. The ζ-potential values were measured in water (pH ~ 5.6) with no added electrolyte.

bonds between the MS templates and the PE building blocks can be selectively formed through cross-linking of amine groups (in the template) and the carboxylic groups (in the PE deposited), either by chemical or thermal means.

Nitrogen sorption measurements were conducted to follow the variation in surface area and porosity of the APTS-BMS spheres as a result of PE deposition. PAA and PAH with molecular weights of 2 000 and 15 000 g mol^{-1}, respectively, were used. Both PAA and PAH were deposited from high salt (0.7 M NaCl) solutions at concentrations of 5 mg mL^{-1} and pH 2.9 and 4.3, respectively. (NaCl was used to facilitate the infiltration of PE in the mesopores, see later in the text.) The samples were heated after deposition of each layer to effect cross-linking. The native APTS-BMS has a surface area of 465 $m^2\ g^{-1}$ and a pore volume of 1.33 $cm^3\ g^{-1}$. After the first layer of PAA infiltration, the surface area and pore volume of the particles significantly decreased to 284 $m^2\ g^{-1}$ and 0.88 $cm^3\ g^{-1}$, respectively. This is attributed to the high PAA loading and blocking of some of the mesopores.

Deposition of subsequent PAH and PAA layers resulted in a surface area decrease of approximately 40 $m^2\ g^{-1}$ per bilayer. The hysteresis loop shifted to slightly lower relative pressure (see Supporting Information, S1) and the center distribution of the large mesopores of the APTS-BMS templates (27 nm) decreased to 22 nm after deposition of three PE layers (PAA/PAH/PAA; data not shown), suggesting PE infiltration in the large mesopores. This finding is supported by FTIR data we previously reported on the same system.[24] No significant variation of the distribution for the smaller mesopores was observed.

We next sought to probe the amount of PAA/PAH infiltrated into the APTS-BMS spheres. For this purpose, we chose to use TGA because it permits quantification of the total amount of both PEs in the APTS-BMS spheres. (FTIR yields information on PAA but overlapping bands make calculation of the adsorbed amount of PAH difficult.[24]) In this case, the higher M_w PAA (30 000 g mol^{-1}) was used, in conjunction with PAH (M_w 15 000 g mol^{-1}), to examine whether the larger PAA can also infiltrate the mesopores. Cross-linking was also performed by heating after deposition of each PE layer. The amount of PE deposited in each infiltration step was determined by measuring the weight loss of the PE-loaded samples in the temperature range of 200−500 °C with reference to the APTS-BMS templates. The total amount of polymer deposited in the MS particles increases with PE layer number, although the amount adsorbed per layer decreases with increasing layer number (Figure 4a). Similar to what is observed for the PAA M_w 2 000 g mol^{-1}/PAH M_w 15 000 g mol^{-1} system by BET (see above) and FTIR,[24] this trend is attributed to increased blockage of the mesopores in the APTS-BMS templates with increasing PE layer number. Experiments using APTS-HMS spheres indicate that PE infiltration occurs in the larger mesopores (10−40 nm) of APTS-BMS. The APTS-HMS spheres (pore size 2.3 nm, see Table 1) were not suitable templates for the generation of NPS: four bilayers of PAA (PAA M_w 2 000 g mol^{-1}, pH 2.9, 0.7 M NaCl) and PAH (PAH M_w 15 000 g mol^{-1}, pH 4.3, 0.7 M NaCl) were deposited onto the APTS-HMS particles with heat-induced cross-linking after deposition of each PE layer. After template removal with HF, only hollow capsules were obtained (see Supporting Information, S2), suggesting that the PAA and PAH do not infiltrate mesopores in this size range but are primarily restricted to the surface of the spheres.[23] We note that mesopores of this size are able to be accessed by small molecules (i.e., dyes) but not by biomacromolecules (i.e., proteins).[22b]

The successive infiltration of PE in the mesopores of APTS-BMS was further demonstrated by CLSM by using fluorescently labeled PAH (FITC-PAH) as the final layer deposited. The APTS-BMS particles were infiltrated with two (PAA/FITC-PAH), four (PAA/PAH/PAA/FITC-PAH), and six ($(PAA/PAH)_2$/PAA/FITC-PAH) layers. In all cases, the CLSM images revealed bright particles with a homogeneous distribution of FITC-PAH throughout the MS template spheres. Figure 4b shows a representative image for the APTS-BMS particles infiltrated with ($(PAA/PAH)_2$/PAA/FITC-PAH), indicating that, within the resolution of optical microscopy, PE infiltration occurs homogeneously throughout the porous particles even after six deposition steps.

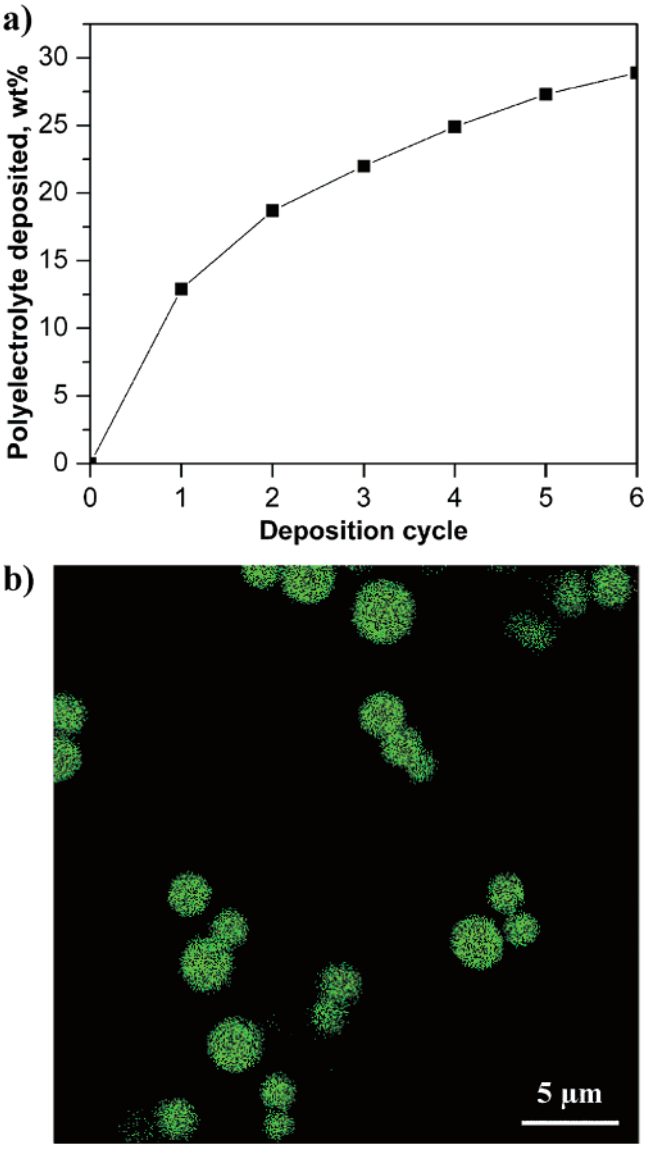

Figure 4. (a) Amount of PE adsorbed as a function of the number of PE infiltration steps ("layer number"). Layers 1, 3, and 5 correspond to PAA (30 000 g mol^{-1}) deposition, and layers 2, 4, and 6 correspond to PAH (15 000 g mol^{-1}) deposition. The data were determined by TGA, and the APTS-BMS template mass was normalized to 100%. (b) CLSM image of APTS-BMS spheres after infiltration of six PE layers ($(PAA/PAH)_2$/PAA/FITC-PAH). PAA and PAH were deposited from 5 mg mL^{-1} solutions containing 0.5 M NaCl. The pH of each PE solution was adjusted to 4.5. Cross-linking of the PEs was achieved by heating the samples at 160 °C for 2 h.

The surface charge characteristics of the PAA/PAH-loaded APTS-BMS particles and the resulting PAA/PAH NPS were examined by microelectrophoresis measurements. The isoelectric points (IEPs) of the different particles were determined from ζ-potential−pH titration experiments (Figure 5). The IEP for particles infiltrated with one layer of PAA was ∼4, a value in close agreement with previous reports for PAA-coated particles.[28] This shows that PAA adsorbed on the APTMS−BMS particles dictates the surface charge properties. Infiltration of the second layer, PAH,

(28) (a) Kato, N.; Schuetz, P.; Fery, A.; Caruso, F. *Macromolecules* **2002**, *35*, 9780. (b) Burke, S. E.; Barrett, C. J. *Langmuir* **2003**, *19*, 3297.

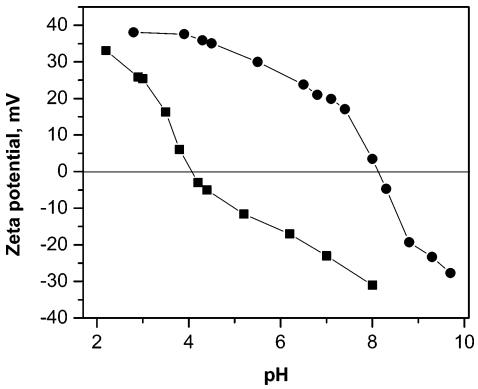

Figure 5. ζ-potential titration curves of PAA- (squares) and PAA/PAH- (circles) infiltrated APTS-BMS particles. PAA (30 000 g mol^{-1}) and PAH (15 000 g mol^{-1}) were deposited from 5 mg mL^{-1} solutions containing 0.5 M NaCl. The pH of each PE solution was adjusted to 4.5. Cross-linking of the PEs was achieved by heating the samples at 160 °C for 2 h.

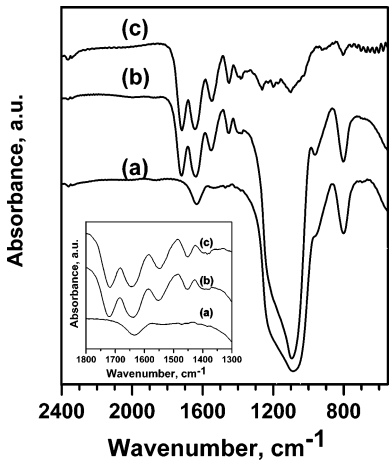

Figure 6. FTIR spectra of (a) APTS-BMS spheres, (b) $(PAA/PAH)_2$/PAA-infiltrated APTS-BMS spheres, and (c) $(PAA/PAH)_2$/PAA NPS obtained after silica template removal with 5 M HF. PAA (2 000 g mol^{-1}) and PAH (15 000 g mol^{-1}) were deposited from 5 mg mL^{-1} solutions containing 0.7 M NaCl at pH 2.9 and 4.3, respectively. Cross-linking was applied after the deposition of each layer by heating the samples at 160 °C for 2 h.

yielded particles with an IEP of ∼8, which is close to the pK_a of PAH,[29] confirming PAH adsorption.

APTS-MS Template Removal. Removal of the APTS-BMS template was proven by both FTIR and EDX analysis. Figure 6 shows FTIR spectra of the APTS-BMS template, five-layer cross-linked ($(PAA/PAH)_2$/PAA)-loaded APTS-BMS spheres, and five-layer cross-linked $(PAA/PAH)_2$/PAA NPS. Silica peaks (800, 960, and 1100 cm^{-1})[30] are observed in the APTS-BMS template (spectrum a) and the template after PAA/PAH assembly (spectrum b). These peaks are greatly reduced in the $(PAA/PAH)_2$/PAA NPS (spectrum c), confirming removal of the silica template. The peaks at 1720, 1570, and 1400 cm^{-1} (spectra b and c) are attributed to the −COOH carbonyl and −COO$^-$ asymmetric and symmetric stretches of PAA, respectively.[29a,31] The presence of non-ionized acid groups in the PAA chains is attributed to the low assembly pH and partial cross-linking.[32] The absorption band at 1635 cm^{-1} can be assigned to the Si−OH vibrations[33] and the N−H bending (scissoring) vibrations of PAH.[27] This peak masks the amide band due to cross-linking (peak at ∼1670 cm^{-1}). In agreement with the FTIR measurements, EDX data showed that only a small amount of silicon (0.8%) was present after removal of the MS template (see Supporting Information, S3). This small amount of silicon is possibly due to the silicon−alkyl groups, which are stable in the presence of HF, and are introduced into the sample through the APTS modification of the BMS particles.[34] Another possibility is the small amount of dissolved silica species (i.e., SiF_6^{2-}) present as a result of the silica template removal step.[35]

Morphology of PAA/PAH NPS. The morphology and porosity of the NPS were examined by SEM and TEM. Figure 7a shows that the $(PAA/PAH)_2$/PAA NPS range in size from 1.2 to 1.9 μm and are spherical, with pores evident in their surface (Figure 7a, inset). These NPS retain the original shape of the BMS templates and do not show signs of collapse, as is commonly observed for PE capsules. TEM confirms that the NPS are spherical (Figure 7b) and nanoporous, as evidenced for the ultramicrotomed samples (Figure 7b, inset). In agreement with the CLSM data (Figure 4b), the TEM image (Figure 7b, inset) shows the homogeneous distribution of the PEs in the interior of the NPS, confirming the effective infiltration of the PEs into the APTS-BMS spheres. The disordered pore structure, with pore sizes of 5−40 nm, is also apparent in Figures 7a (inset) and 8b (inset). NPS were also prepared if the low molecular weight PAA (2 000 g mol^{-1}) was replaced by higher molecular weight PAA (30 000 g mol^{-1}) (Figure 7c,d).

As the LbL method is largely independent of substrate morphology, we applied the method to prepare nanoporous polymer-based fibers (NPF) by using MS templates with fiber morphologies. The fibers are about 1 μm in diameter and 10−30 μm in length and have similar porosity to the BMS spheres used.[26] Four layers of PE were infiltrated into the fibers, PAA (2 000 g mol^{-1}) and PAH (15 000 g mol^{-1}), and the samples were heated after each layer was deposited to effect cross-linking. Figure 8 shows the PAA/PAH NPF at different magnifications after silica removal. The polymeric fibers have lengths of tens of micrometers and diameters of hundreds of nanometers, closely mimicking the morphology of the MS fibers. SEM images show that pores in the vicinity of 5−50 nm are present on the surface of the NPF (data not shown). Preparation of these structures demonstrates that the PE-infiltration-MS template synthesis provides a facile method to prepare nanoporous materials with different morphologies.

Effect of Preparation Parameters. *(a) Cross-Linking.* Cross-linking of each PE layer was performed by heating

(29) (a) Harris, J. J.; DeRose, P. M.; Bruening, M. L. *J. Am. Chem. Soc.* **1999**, *121*, 1978. (b) Schuetz, P.; Caruso, F. *Adv. Funct. Mater.* **2002**, *13*, 929.
(30) Inaki, Y.; Yoshida, H.; Yoshida, T.; Hattori, T. *J. Phys. Chem. B* **2002**, *106*, 9098.
(31) Stair, J. L.; Harris, J. J.; Bruening, M. L. *Chem. Mater.* **2001**, *13*, 2641.
(32) Yoo, D.; Shiratori, S. S.; Rubner, M. F. *Macromolecules* **1998**, *31*, 4309.
(33) Takahashi, R.; Sato, S.; Sodesawa, T.; Kawakita, M.; Ogura, K. *J. Phys. Chem. B* **2000**, *104*, 12184.
(34) (a) Choi, J.; Harcup, J.; Yee, A. F.; Zhu, Q.; Laine, R. M. *J. Am. Chem. Soc.* **2001**, *123*, 11420. (b) Costa, R. O. R.; Vasconcelos, W. L. *Macromolecules* **2001**, *34*, 5398.
(35) Dähne, L.; Baude, B.; Voigt, A. Patent WO 2004/014540 A1, 2003.

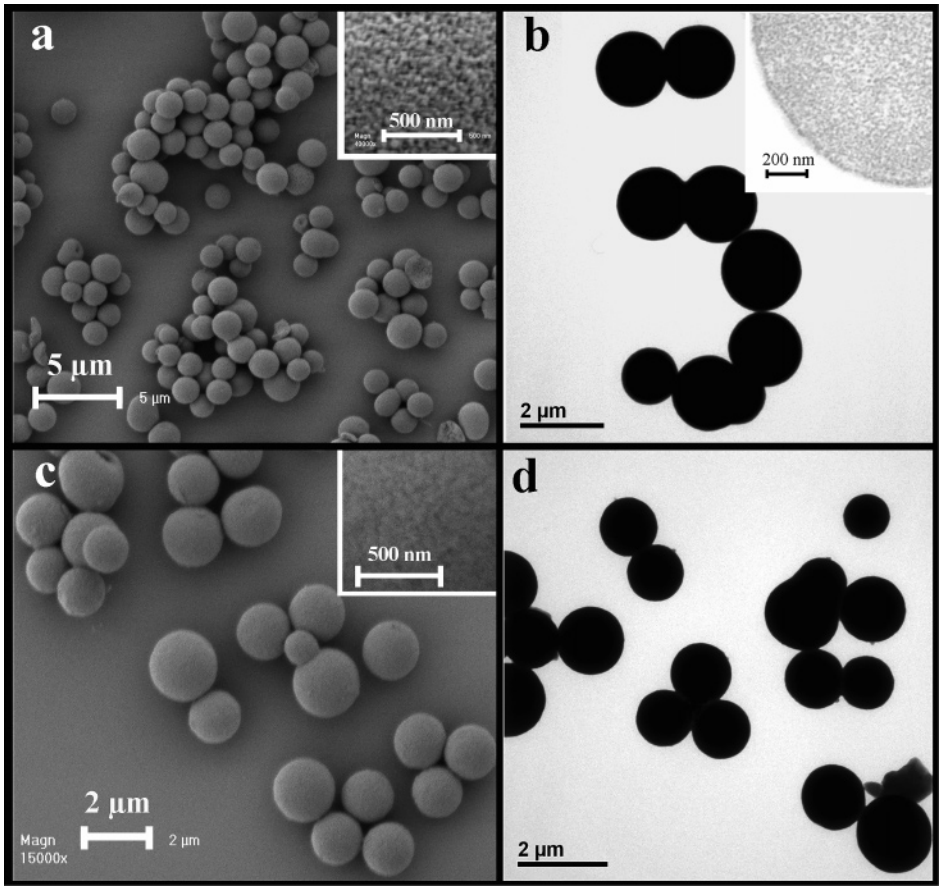

Figure 7. SEM (a) and TEM (b) images of the $(PAA/PAH)_2/PAA$ NPS. PAA (2 000 g mol^{-1}) and PAH (15 000 g mol^{-1}) were deposited from 5 mg mL^{-1} solutions containing 0.7 M NaCl at pH 2.9 and 4.3, respectively. Cross-linking was applied after the deposition of each layer by heating the samples at 160 °C for 2 h. SEM (c) and TEM (d) images of the PAA/PAH NPS. PAA (30 000 g mol^{-1}) and PAH (15 000 g mol^{-1}) were deposited from 5 mg mL^{-1} solutions containing 0.5 M NaCl. The pH of each PE solution was adjusted to 4.5. Cross-linking was applied after the deposition of each layer by heating the samples at 160 °C for 2 h. The insets of parts a and c are higher magnification images; the inset of part b is an ultramicrotomed thin section (∼90 nm thickness) of the NPS.

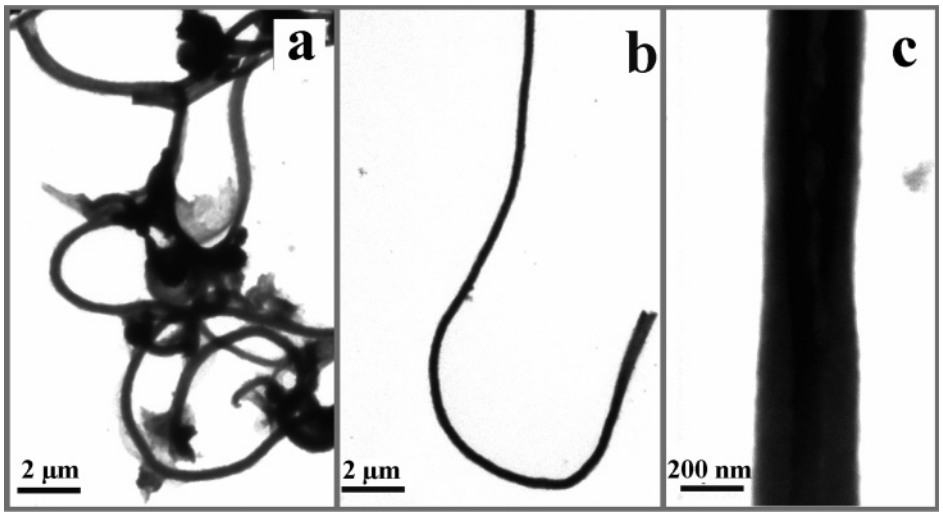

Figure 8. TEM images of the $(PAA/PAH)_2$ NPF at different magnifications. PAA (2 000 g mol^{-1}) and PAH (15 000 g mol^{-1}) were deposited from 5 mg mL^{-1} solutions containing 0.7 M NaCl at pH 2.9 and 4.3, respectively. Cross-linking was applied after the deposition of each layer by heating the samples at 160 °C for 2 h.

the air-dried samples at 160 °C for 2 h. The deposition of two PE (i.e., PAA/PAH) layers was investigated, and the cross-linking treatment was selectively applied to either or both layers. NPS were not obtained in the absence of cross-linking. In contrast, if the cross-linking process was applied *only* in the second step, that is, after the infiltration of PAA and PAH, deformed spheres were obtained (data not shown). This is possibly caused by competitive binding between PAH and the amine groups anchored to the silica surface for the preloaded PAA, which would result in the formation of PAA−PAH complexes in solution or on the particle surface. Such effects ("PE stripping") have been previously observed, especially for low molecular weight PEs.[36] It is also possible that without cross-linking the PEs migrate to the particle

surface, favoring the formation of capsule-like materials (see later in the text). However, cross-linking after infiltration of each PE yields stable PAA/PAH NPS, even with only two PE (PAA and PAH) infiltration steps, thus enhancing the structural stability of the NPS (see Figure 7c,d).[29] An alternative approach for the formation of amide bonds is by using EDC as an activator.[37] The carboxylate moiety in PAA reacts with the diimide groups and forms an activated species, which in a second step reacts with the amines in PAH or the APTS-BMS templates to form the amide bonds. EDC-induced cross-linking at room temperature makes this method promising for the synthesis of bioactive materials, in which high temperatures are to be avoided to prevent denaturing the biomolecules. No apparent morphological differences in the NPS were observed between the heating and the EDC-induced cross-linking protocols. We note that cross-linking using EDC permits the formation of nanoporous polymeric materials with potentially controlled mechanical stability,[29b] which should be of interest in the design of NPS where both particle integrity and responsiveness are necessary, such as for biomaterials and controlled-release applications.

(b) PE Solution pH. Because both PAA and PAH are weak PEs, that is, the ionization of the PE is dependent on the pH,[38] the influence of pH was investigated by separately changing the solution pH of one PE and fixing the other. NPS can be prepared with a pH range of 2−6 for PAA, with the pH of PAH fixed at 4.5. If the PAA deposition solution had a pH < 1 or > 7, only ruptured capsule-like products were obtained after silica removal. This is rationalized by the PAA ($pK_a \sim 4.3$)[28] having an increased charge density at higher pH, thereby adopting a more extended conformation and being spatially restricted and thus adsorbing outside of the nanopores. PAA has a reduced charge density at lower pH (i.e., pH 2−6), thereby adopting a more coiled conformation and adsorbing in greater amounts. With further decreasing the pH, more of the carboxylic acid groups become protonated, reducing electrostatic association of PAA and the APTS-modified BMS template. The pH influence of PAH ($pK_a \sim 8-10$)[38] was also investigated by fixing the pH of the PAA solution at 4.5. Intact PAA/PAH NPS were prepared provided the PAH solution had a pH between ∼4 and ∼8.5. In contrast, capsule-like products were obtained at a PAH solution pH of 2.5 (see Supporting Information, S4), suggesting the adsorption of PAH is mainly restricted to the particle surface at lower pH.

(c) PE Solution Ionic Strength. The ionic strength of the deposition solutions was found to significantly influence the preparation of the NPS because, like solution pH, it influences both the conformation and charge density of the weak PEs. PEs typically have a more coiled morphology in solution as the salt concentration increases.[39] We specifically chose PAA and PAH with higher molecular weights as we expected to see a more pronounced influence of salt on larger molecular weight PEs. The presence of salt (0.5 M NaCl) in both the PAA (M_w 30 000 g mol^{-1}) and PAH (M_w 70 000 g mol^{-1}) deposition solutions yielded intact PAA/PAH NPS (Figure 9a), suggesting the highly coiled PE conformation promoted by the presence of salt favors PE infiltration into the mesopores. Decreasing the salt concentration in the PAH deposition solution to 0.15 M NaCl (while keeping the PAA ionic strength at 0.5 M) resulted in deformed (partly collapsed) NPS (Figure 9b). The density of the NPS further decreased if PAH solutions of lower ionic strength (0.05 M NaCl) were used, as seen by the lower electron contrast in the products (Figure 9c). Further, only capsule-like products were obtained when no salt was added to the PAH deposition solution (Figure 9d). This can be explained by the fact that, in the low ionic strength solution, the PAH assumes a more extended conformation and contains less loops and tails because charges on the chain are less screened than when higher amounts of salt are present. Consequently, PE infiltration into the mesopores is largely restricted. This finding was verified by CLSM, where only a faint fluorescent ring was observed from the APTS-BMS particles when the FITC-labeled PAH was deposited in the absence of salt (data not shown). We also observed a similar salt dependency for the case of lower molecular weight PAA (M_w 2 000 g mol^{-1}) and PAH (M_w 15 000 g mol^{-1}; see Supporting Information, S5).

Tailoring the Composition of NPS. A main advantage of the approach proposed is that it offers a general and versatile route to the preparation of NPS of diverse and tailored composition. Herein, we demonstrate that it can be applied to the preparation of NPS containing copolymers, peptides, proteins, and small molecules.

(a) Copolymer-Based NPS. Using copolymers that comprise both weak and strong PE pendant groups may remove the need for chemical cross-linking to improve the stability of weak PE multilayers.[40] We infiltrated a copolymer containing both weakly and strongly charged pendant groups, PSSMA (Figure 1), in alternation with PAH, in the APTS-BMS spheres. The strongly charged groups (SS) are expected to form electrostatic linkages (to enhance film stability), while the weakly charged carboxylic groups (MA) can associate with the APTS-modified silica substrates and form chemical bonds after cross-linking. PSSMA with SS/MA mole ratios of 1:1 and 3:1 were used. The NPS were prepared from two PE infiltration steps, in the order PSSMA and PAH. The copolymer-based NPS (i.e., PSSMA/PAH NPS) were prepared according to the standard method used for the PAA/PAH NPS synthesis, with the exception that only the first PSSMA layer was cross-linked to the APTS-BMS surface by heating, but the subsequently deposited PE layers were not cross-linked. Aggregated and collapsed NPS were obtained when PSSMA 1:1 was used. In contrast, intact spheres were found when PSSMA 3:1 was employed (Figure 10a), indicating that the PSSMA 3:1/PAH complex is more stable after silica removal compared with PSSMA 1:1/PAH. This can be rationalized by the enhanced electrostatic interactions between PSSMA 3:1 and the amine groups of PAH. It is worth noting that, unlike the PAA/PAH system, no cross-

(36) Sui, Z.; Salloum, D.; Schlenoff, J. B. *Langmuir* **2003**, *19*, 2491.
(37) Hermanson, G. T.; Mallia, A. K.; Smith, P. K. *Immobilized Affinity Ligand Techniques*; Academic Press: London, 1992.
(38) Shiratori, S. S.; Rubner, M. F. *Macromolecules* **2000**, *33*, 4213.
(39) Dubas, S. T.; Schlenoff, J. B. *Macromolecules* **1999**, *32*, 8153.
(40) Tjipto, E.; Quinn, J. F.; Caruso, F. *Langmuir* **2005**, *21*, 8785.

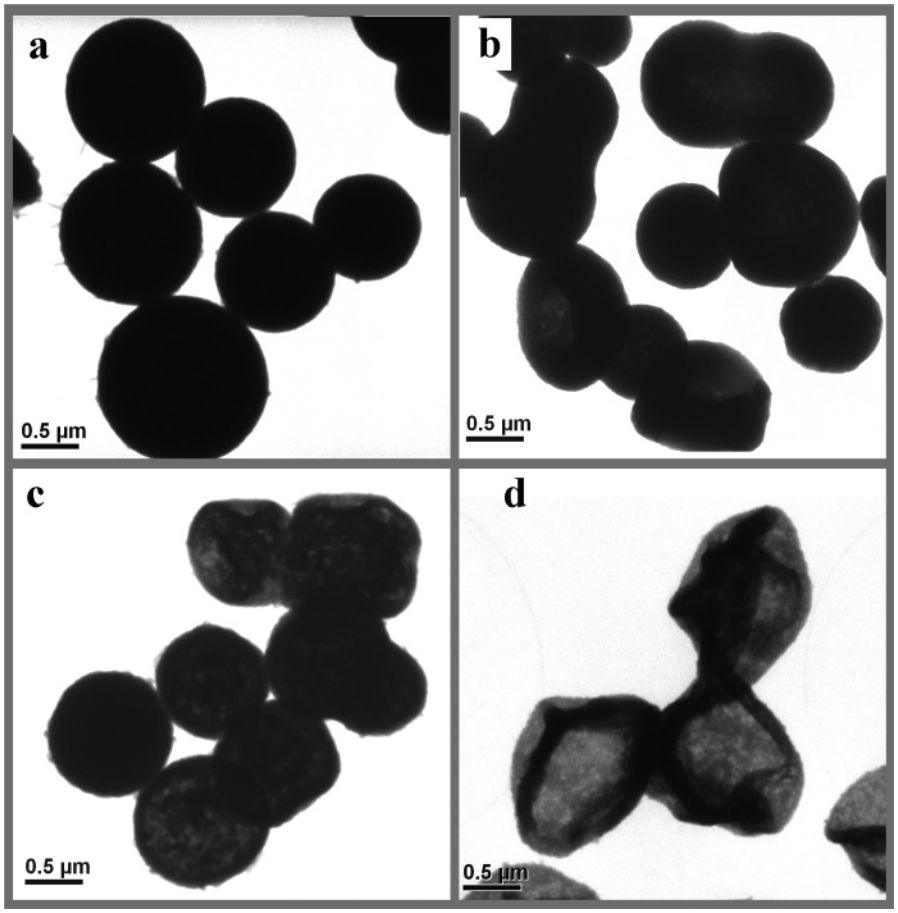

Figure 9. TEM images of the PAA/PAH NPS prepared with PAH (M_w 70 000 g mol^{-1}) solutions containing (a) 0.5 M, (b) 0.15 M, (c) 0.05 M, and (d) 0 M NaCl and PAA (M_w 30 000 g mol^{-1}) solutions containing 0.5 M NaCl. In all cases the PAH and PAA solution pH values were fixed at 4.5. Cross-linking was applied after the deposition of each layer by heating the samples at 160 °C for 2 h.

linking between the PSSMA and PAH layers is necessary to obtain these NPS. We also examined the ability of the homopolymer poly(styrenesulfonate) (PSS) (M_w 70 000 g mol^{-1}, 5 mg mL^{-1}, pH 4.5, 0.5 M NaCl) and PAH (M_w 15 000 g mol^{-1}, 5 mg mL^{-1}, pH 4.5, 0.5 M NaCl) to form NPS. In this case, only capsule-like products were obtained (see Supporting Information, S6). This is likely caused by desorption of the PSS upon exposure to the second deposition solution (PAH), because the PSS cannot be cross-linked with the MS template. The competitive binding between PAH and the amine groups anchored to the silica surface for the preloaded PSS is likely to result in the formation of PSS−PAH complexes in solution and/or on the particle surface, leading to the capsule materials obtained. The above data highlight the importance of chemically cross-linking the first layer with the template surface to generate porous replica polymer-based structures. The ability to form NPS from copolymers represents a significant step, as monomer units with different properties and diverse functional groups can be readily incorporated into the chain, and the proportion of each unit varied by changing the copolymer composition. Such materials add a level of sophistication to the NPS beyond those prepared simply from homopolymeric materials.

(b) Nanoporous Peptide Particles. There is increasing interest in preparing designed materials composed of biomacromolecules (i.e., peptide, protein) with defined morphologies because of their relevance in catalysis, sensing, and drug delivery. Peptides in the form of nanofibrils,[41] nanotubes,[42] and spherical assemblies[43] have been prepared by various methods, including self-assembly, acid−base chemistry, and precipitation in organic solvents.[41−43] We sought to apply our method to prepare peptide NPS. Nanoporous peptide spheres were prepared through the sequential deposition of PGA and PLL in the APTS-BMS templates. To enhance the stability of the PGA/PLL layers, cross-linking using EDC was performed to form amide bonds between the −COOH groups (in PGA) and the $-NH_2$ moieties in PLL. Intact PGA/PLL NPS (Figure 10b) were obtained after removing the silica template by HF. We also prepared hybrid PE/polypeptide particles, including PGA/PAH and PAA/PLL NPS by using the same procedure (data not shown). These nanoporous peptide and hybrid-peptide particles are appealing supports or vessels for the loading of biomolecules or drug substances. We are currently investigating the uptake of proteins and drugs in these particles.

(41) (a) Mesquida, P.; Ammann, D. L.; MacPhee, C. E.; McKendry, R. A. *Adv. Mater.* **2005**, *17*, 893. (b) Kaneko, T.; Higashi, M.; Matsusaki, M.; Akagi, T.; Akashi, M. *Chem. Mater*. **2005**, *17*, 2484.
(42) Couet, J.; Samuel, J. D. J. S.; Kopyshev, A.; Santer, S.; Biesalski, M. *Angew. Chem., Int. Ed.* **2005**, *44*, 2.
(43) (a) Cha, J. N.; Birkedal, H.; Bartl, M. H.; Deming, T. J.; Stucky, G. D. *J. Am. Chem. Soc*. **2003**, *125*, 8285. (b) McKenna, B. J.; Birkedal, H.; Bartl, M. H.; Deming, T. J.; Stucky, G. D. *Angew. Chem., Int. Ed.* **2004**, *43*, 5652.

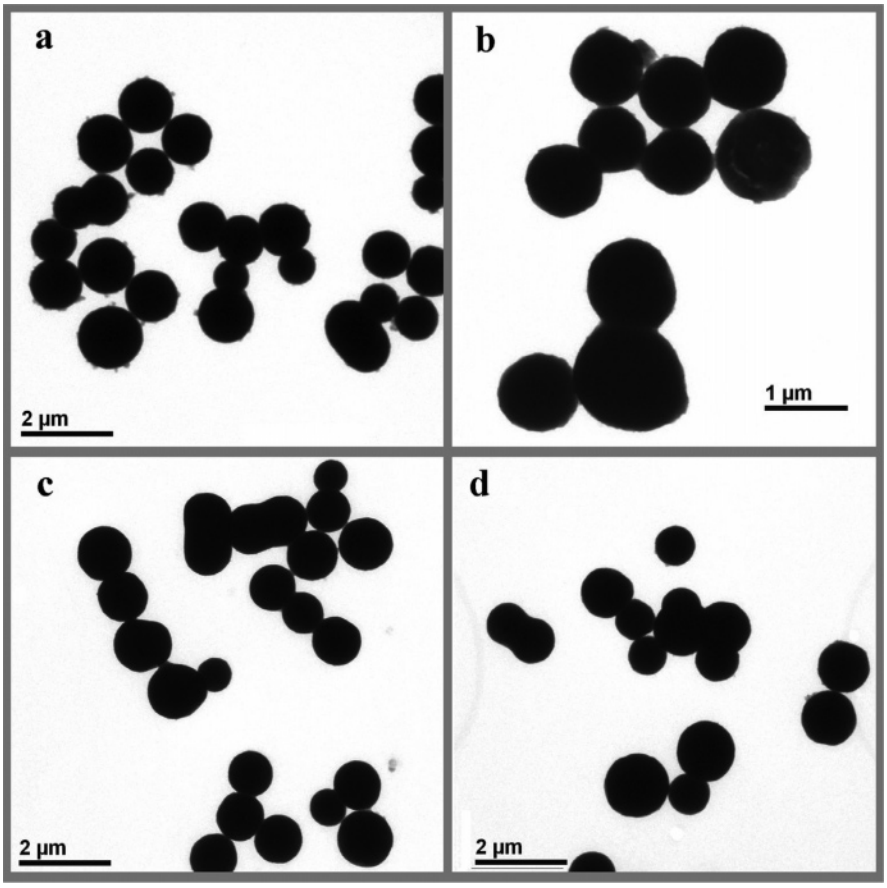

Figure 10. TEM images of the (a) PSSMA 3:1/PAH NPS, (b) PGA/PLL NPS, (c) PAA/lysozyme NPS, and (d) PGA/EDA NPS pairs. Only the first layer of PSSMA was cross-linked with the MS substrate in sample a. EDC-induced cross-linking was performed after deposition of each PE layer in samples b−d. The pH and salt concentrations for the deposition solutions were 3.8, 0.3 M (PSSMA); 4.5, 0.3 M (PGA); 4.5, 0.3 M (PLL); 4.5, 0.5 M (PAH); and 4.5, 0.5 M (PAA). Lysozyme was dissolved in 50 mM PB at pH 7.0 with a concentration of 5 mg mL^{-1}. EDA was dissolved in water at a concentration of 60 mg mL^{-1}. Two layers were deposited in all of the samples.

(c) Nanoporous Protein Particles. To prepare the nanoporous protein particles, PAA was first infiltrated into the APTS-BMS particles and subsequently cross-linked with the amine groups grafted on the MS templates. The PAA-infiltrated particles were then dispersed in the protein solution (5 mg mL^{-1} of lysozyme in 50 mM PB at pH 7.0) and incubated for 72 h. Because lysozyme has an IEP of ∼11, under these conditions lysozyme is likely to electrostatically interact with PAA. The amount of protein immobilized (20 wt % of the MS template) was determined by monitoring the difference in the protein absorbance (280 nm) in solution before and after adsorption. Excess lysozyme was removed by two cycles of centrifugation and washing with 50 mM PB. To enhance the stability of the PAA/protein layers, cross-linking using EDC was performed to form amide bonds between the $-COOH$ groups (in PAA) and the $-NH_2$ moieties in the protein. Intact PAA/lysozyme particles (Figure 10c) were obtained after removing the silica template by HF. The PAA/lysozyme NPS has a lysozyme/PAA composition of ∼1:1 (w/w), that is, about 50 wt % of the particle is protein. The protein content is less than that of the nanoporous protein particles (NPS-lyz) we recently reported, in which particles with a protein content as high as 83 wt % were obtained.[22d] In that work,[22d] lysozyme was first infiltrated in BMS particles and then bridged through cross-linking with PAA. This indicates that infiltrating PAA first causes some pore blockage and that less lysozyme is loaded; however, the formation of the NPS shows that sufficient lysozyme can effectively infiltrate into the PAA-loaded mesopores and associate with PAA to form a robust structure after cross-linking. Exposing the cross-linked PAA/lysozyme NPS to pH 2.0, conditions where lysozyme rapidly desorbs if not cross-linked to PAA,[22c] showed negligible protein loss. This suggests that this approach is useful for protein immobilization in porous materials.

(d) PE/Small Molecule NPS. We examined the possibility of preparing NPS from PEs and small molecules such as EDA. The EDA is a short molecule (M_w 60 g mol^{-1}) that contains two amine groups (Figure 1). PAA or PGA was first infiltrated and then heat cross-linked with the APTS-BMS template. A total of 20 mg of the PE-loaded particles was then dispersed in 2 mL of EDA solution with a concentration of 60 mg mL^{-1} and stirred for 2 h. After four cycles of washing with water to remove excess EDA, EDC cross-linking, and template removal, spherical PGA/EDA NPS (Figure 10d) or PAA/EDA NPS (data not shown) with diameters between 0.8 and 1.1 μm were obtained. Control experiments showed that NPS were not formed if the EDA infiltration step was eliminated, even if EDC cross-linking was performed on the PAA-loaded APTS-BMS spheres. This indicates that EDA plays an essential role in connecting/binding the polymers together.

NPS Protein Loading and Release. We previously reported that NPS can be used to sequester proteins, leading

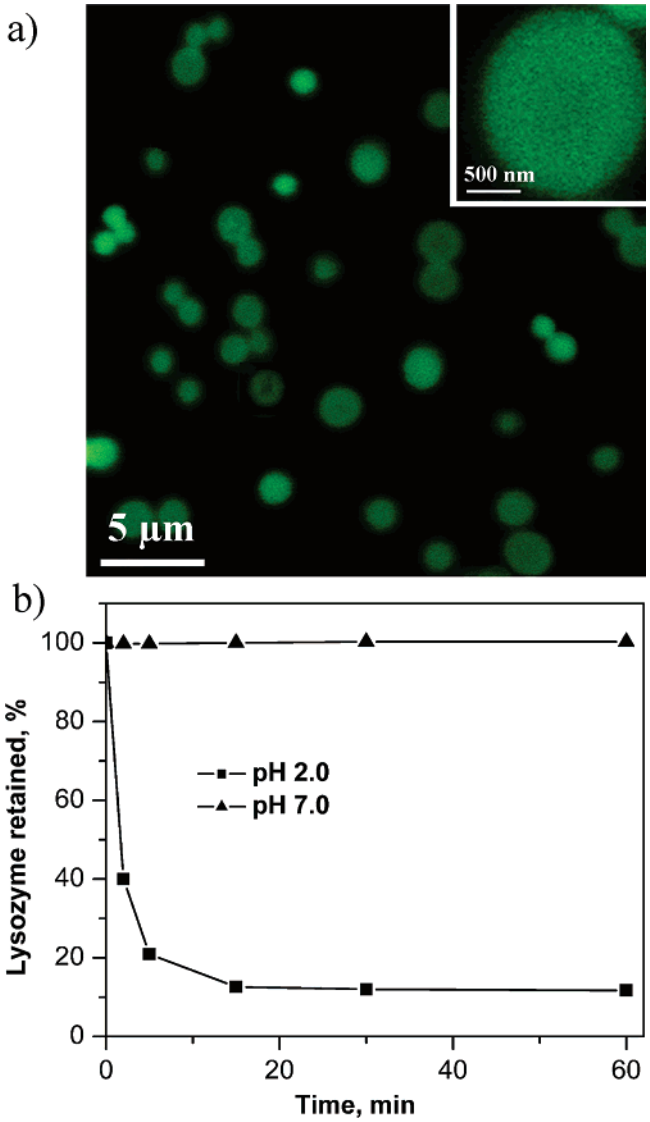

Figure 11. (a) CLSM images of $(PAA/PAH)_2/PAA$ NPS after FITC-labeled lysozyme immobilization. The inset is a higher magnification image. (b) Enzyme release properties of the $(PAA/PAH)_2/PAA$ NPS. PAA (2 000 g mol^{-1}) and PAH (15 000 g mol^{-1}) were deposited from 5 mg mL^{-1} solutions containing 0.7 M NaCl at pH 2.9 and 4.3, respectively. Cross-linking was applied after the deposition of each layer by heating the samples at 160 °C for 2 h.

to high protein loadings.[24] For example, cross-linked $(PAA/PAH)_2/PAA$ NPS readily adsorb lysozyme, resulting in the NPS being composed of ~90 wt % lysozyme after incubation of the NPS in a lysozyme solution for 60 min. This corresponds to a concentration of about 470 mg mL^{-1} of lysozyme in NPS. Figure 11a shows a representative CLSM image of the lysozyme-loaded NPS. We investigated the stimuli-responsive release of the protein-loaded NPS by varying the pH of the surrounding medium. At pH 7, lysozyme is positively charged and is expected to electrostatically associate with the negatively charged $(PAA/PAH)_2/PAA$ NPS. (An IEP of ~5.3 was obtained for the $(PAA/PAH)_2/PAA$ NPS—data not shown.) TGA data shows that the spheres are composed of more PAA than PAH (Figure 4), so the excess PAA charges are likely to interact with the lysozyme. Under pH 7 conditions, no protein leakage was observed over 60 min. When the particles were dispersed in 50 mM PB at pH 2.0, about 80% of the lysozyme was released from the NPS within 5 min, and almost 90% was released after 60 min (Figure 11b). At pH 2, it is expected that there will be diminished electrostatic interactions, as both the protein and the NPS are positively charged. The protein loading ability of NPS was fully recovered after several washing cycles with pH 7.0 PB. The NPS showed no apparent loss of enzyme loading capacity, even after six successive loading (pH 7) and release (pH 2) experiments, showing that they represent stable stimuli-responsive systems that can effectively sequester high concentrations of protein and release the protein when stimulated.

Conclusions

A versatile approach, based on sequential assembly and MS templating, was used for the preparation of polymer-based nanoporous materials. This method affords NPS of diverse composition (PEs, peptides, proteins, and small molecules) and morphology (spheres and fibers). Infiltration of the materials in the mesopores was proven by gas sorption, TGA, CLSM, SEM, and TEM. Electron microscopy data confirmed that the NPS have pores ranging from about 5−50 nm. The pH and ionic strength of the PE deposition solutions play an essential role in the NPS synthesis. Coiling of the PEs, which is largely influenced by pH and ionic strength, promotes PE infiltration in the mesopores and the subsequent formation of intact NPS. Cross-linking between the PEs and the template surface is, in some cases, required for the generation of stable, nanoporous spheres. It is postulated that unless the first layer is immobilized, competing interactions between incoming PE and the preadsorbed material result in loss of material from within the pores. The interaction between the PE pairs is also important in the synthesis. Cross-linking of weak PE pairs (PAA and PAH) is necessary to obtain stable NPS whereas for PE pairs with stronger interaction (e.g., PSSMA 3:1/PAH), cross-linking is not required. As a result of the nanoporosity and large number of functional groups, the NPS show excellent capacity for immobilization of proteins (lysozyme). Reversible loading and release of the NPS particles was achieved simply by varying the pH to mediate the electrostatic association between the proteins and the NPS host. The versatility of this technique will facilitate designing NPS for the uptake of various species such as macromolecules, low molecular weight drugs, pesticides, fragrances, and nanoparticles through, for example, electrostatic association or H-bonding with the NPS host. These systems, with nanaoscale porosity and designed functionality, are envisaged to offer new opportunities for their application in biosensing, catalysis, and drug delivery.

Acknowledgment. This work was supported by the Australian Research Council (Discovery Project and Federation Fellowship Schemes) and the Victorian State Government, Department of Innovation, Industry and Regional Development, Science, Technology and Innovation initiative. The Particulate Fluids Processing Centre is acknowledged for infrastructure support. William Mulholland is thanked for assistance with CLSM experiments, and Elvira Tjipto and John F. Quinn are thanked for helpful discussions.

Supporting Information Available: Nitrogen sorption isotherms of the APTS-BMS spheres with and without PE infiltrated in the pores, electron microscopy images of the polymer samples prepared using MS spheres with a pore size of 2−3 nm as templates, EDX spectra of the PE-infiltrated APTS-BMS spheres before and after silica template removal, TEM images of the PAA/PAH NPS samples prepared with PAH deposition solutions of different pH values and salt concentrations, and a TEM image of the polymer sample prepared by the deposition of PSS/PAH (PDF). This material is available free of charge via the Internet at http://pubs.acs.org.

CM060866P